DOI:10.1021/jf103523u

JOURNAL OF AGRICULTURAL AND FOOD CHEMISTRY
ARTICLE

Characterization of Water Binding and Dehydration in Gelatinized Starch

Xiaowen Lv,[†,‡,∥] Lei Wu,[†,∥] Jing Wang,[§] Junguo Li,[†] and Yuchang Qin*[,†]

[†]Feed Safety Reference Laboratory of the Ministry of Agriculture, Feed Research Institute, Chinese Academy of Agricultural Sciences, Beijing, China, [‡]Key Laboratory of Feed Biotechnology of the Ministry of Agriculture, Feed Research Institute, Chinese Academy of Agricultural Sciences, Beijing, China, and [§]State Key Laboratory of Environmental Chemistry and Ecotoxicology, Research Center for Eco-Environmental Sciences, Chinese Academy of Sciences, Beijing, China. [∥]These authors contributed equally to this work.

Using near-infrared spectroscopy and thermogravimetry coupled with differential scanning calorimetry (TG−DSC), we investigated the characteristics of water in starch and the effects of the inner structure of starch on dehydration. The results directly show that the dehydration process is significantly more favorable in native starch than in gelatinized starch. When the starch was heated to 100 °C, the water retention in gelatinized starch was 22.35 per total water content, much greater than that in native starch (4.3%). The hydrogen bond network that changes from native starch to gelatinized starch was simultaneously explored, and the weaker hydrogen bonds were found to be predominant in the hydrogen bond network of gelatinized starch.

KEYWORDS: Gelatinized starch; native starch; thermogravimetry; water binding; dehydration

INTRODUCTION

The interactions of water molecules in polymers have long been the subject of interest for polymer scientists (*1*−*5*). The molecular level interactions that influence the state of water in macromolecules have been studied by nuclear magnetic resonance (NMR), Raman, infrared, and near-infrared spectroscopies (*6*,*7*). Angell and Rodgers measured the near-infrared spectra of water at various temperatures and suggested a disrupted network model for water described by the exchange of energy between weaker and stronger hydrogen bonds (*8*). According to the disrupted network model, the absorption of water in the near-infrared region is due to two different classes of O−H oscillators, the so-called "weakly hydrogen bonded" and "strongly hydrogen bonded" water oscillators (*9*). Previous studies also proved that the absorption bands of the weaker and stronger hydrogen bonds of water were at 1412 and 1491 nm, respectively (*10*,*11*). Thus, the absorption bands in the near-infrared region are excellent markers of the state of water O−H bonds and hydrogen bonds (*5*). At the same time, a variety of chemometric techniques have been used in the analysis of spectroscopic data; for example, partial least-squares (PLS) regression analysis was successfully used to investigate the hydrogen bond structure and temperature-dependent infrared (IR) spectra of water (*12*).

Starch provides 70−80% of the calories consumed by humans worldwide, and modified starches have an enormous number of industry uses (*13*). Starch exists as granules with both amorphous and crystalline regions (*14*). Water is an integral part of the crystalline unit cell and also serves as a plasticizer of the amorphous regions. The crystallites contain 10% water by mass (*13*), and water molecules have been found to be located between the parallel-stranded double helices of the crystalline part of starch (*15*, *16*). Moreover, previous studies have aimed to examine the distribution and state of water within starch granules (*17*, *18*) and during physical or chemical processing (*19*, *20*). However, for many OH groups and the oxygen atom in the starch chain, it is difficult to study the changes in the hydrogen bond network within starch and to compare the transportation properties of water in different starch products. Furthermore, because of drying kinetics and applications, the effect of changes in the inner structure of starch upon dehydration is quite important to study; however, surprisingly few data are currently available.

The investigation of water binding and related characteristics is critical to exploiting the potential of starch applications and nutritional implications (*21*). Although no universal definition of bound water has been adopted because of the complexity and interaction of the binding forces involved (*22*, *23*), water present in starchy products is classified into monolayer, multilayer, and condensed water. Thermogravimetry coupled with differential scanning calorimetry (TG−DSC) is usually used to measure crystallization and phase changes. TG−DSC could also provide precise water mass loss information along with heat flow data. Moreover, near-infrared spectroscopy (NIRS) could reveal the changes in hydrogen bonds, which form between water and glucose units.

With the techniques of TG−DSC and NIRS, we are interested in investigating how and why the properties of the hydrogen bond network change when the inner structure of starch is transformed by thermal treatment. Moreover, the effects of the inner structure on the properties of starchy products during hydration are also discussed here.

*To whom correspondence should be addressed. Telephone: +86-010-82106058. Fax: 86-010-82106069. E-mail: lewinecn@gmail.com.

 Published on Web 12/02/2010

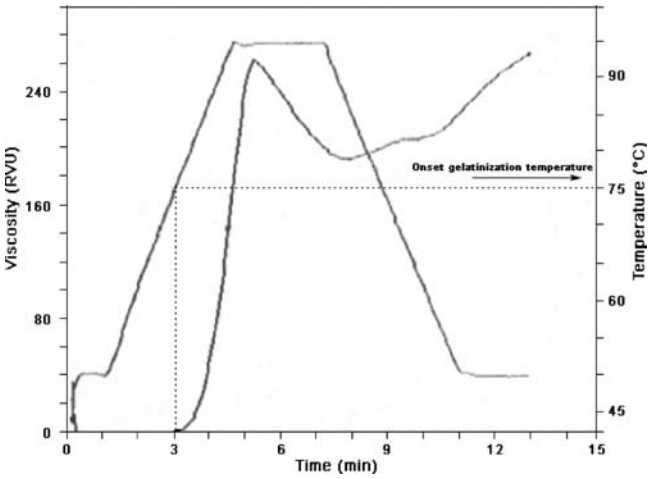

Figure 1. RVA pasting curve for the mixture of native corn starch with 20% starch in the mixture.

MATERIALS AND METHODS

Rapid Visco Analysis (RVA). The pasting temperature of corn starch was determined using an RVA-4 instrument (Newport Scientific Pvt. Ltd., North Ryde, New South Wales, Australia) according to the method of Zaidul et al. (*24*). Corn starch samples were added to 25 mL of distilled water to prepare 20% suspensions on a dry weight basis. Each suspension was kept at 50 °C for 1 min and then heated to 95 °C at a rate of 15 °C/min and held at 95 °C for 2.5 min. They were then cooled to 50 °C at a rate of 15 °C/min and kept at 50 °C for 2 min.

Preparation of Gelatinized Starch Samples. Gelatinized starch samples were obtained from corn starch. Native corn starch (sample I) was slurried in distilled water at a ratio of 1:5. The slurries were heated for 7, 10, and 15 min in a water bath at 70 ± 1 °C and stirred at 200 rpm. To obtain fully gelatinized starch, we heated another slurry for 60 min in a water bath at 100 °C. The slurries were cooled to room temperature and then centrifuged at 1100*g* for 10 min. The slurries were subsequently placed in a freeze-dryer. The freezing process started at −70 °C for 20−30 h. The vacuum level was lower than 1 Pa, and the ampules were sealed by a gas burner to maintain the vacuum. Then, the freeze-dried starch was milled for 20 s using a RETSCH ZM 100 laboratory mill (IKA Labortechnik, Staufen,

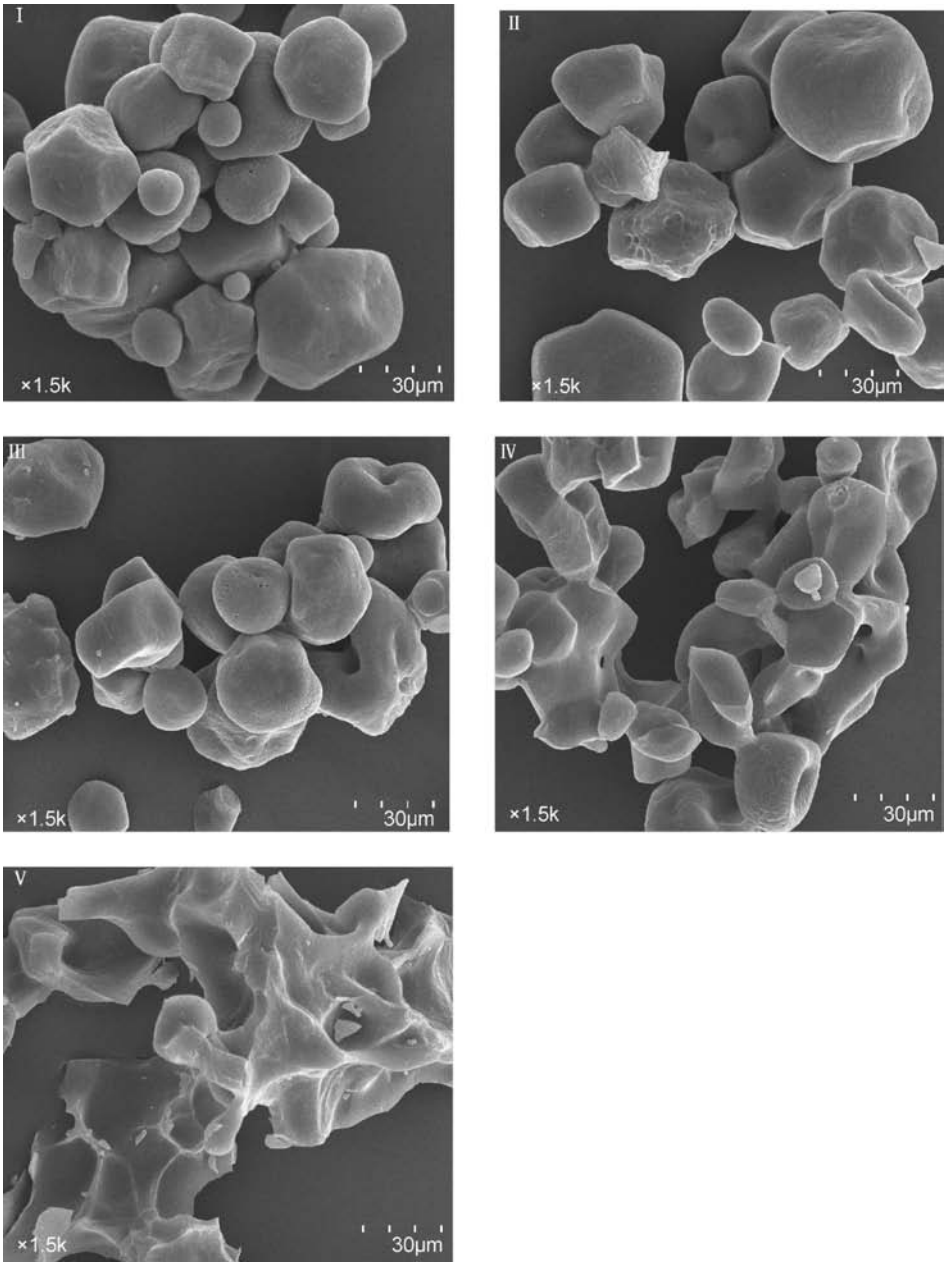

Figure 2. Surface morphologies (1500×) of different starch samples (I−V).

Germany). The powder was sifted through a sieve with a mesh size of 1.0 mm. The degree of gelatinization was measured by the enzymatic method (*25*), and four kinds of gelatinized starch with degrees of gelatinization of 33.4, 51.3, 68.7, and 96.8% (samples II−V, respectively) were obtained using this procedure. These samples were kept at 25 °C above the drying agent in a sealed container for further use.

Scanning Electron Microscopy (SEM). The surface morphology of native starch and each gelatinized starch was observed using a Hitachi S-3400N scanning electron microscope (Hitachi Science Systems, Tokyo, Japan). The starch samples were mounted and coated with gold under vacuum. Pictures were captured using automatic image-capturing software (Hitachi High-Technologies, Pleasanton, CA).

X-ray Diffraction Analysis. X-ray diffraction patterns of native starch and each gelatinized starch were recorded using a Rigaku Dmax-2400 X-ray diffractometer with Cu Kα radiation ($\lambda = 1.5406 \times 10^{-10}$ m) (Rigaku Co.). The measurement conditions were as follows: 40 kV and 100 mA of power, automatic monochromator, 0.5° divergence slit, 0.5° scattering slit, 0.3° receiving slit, continuous scan mode, 3−40° scan range, scan rate of 2.0°/min, and scan step of 0.02°.

TG−DSC Analysis. One aliquot (~1 g) of each starch sample was placed above distilled water in a sealed container kept at room temperature. All samples were moistened until the water content reached a constant concentration (~17% g/g). The moisture content was determined using modified ISO Method 1666, and the samples were dried in an oven at 130 °C for 4 h (*26*). Then, each sample was analyzed by TG−DSC (Q600, TA Instruments) with each treatment performed in triplicate. Data from the TG−DSC analysis were subjected to standard deviation analysis.

A platinum cup was used in the TG−DSC test, and the weight of each sample was constant at 15 ± 0.1 mg. Scans were collected at a constant rate of heating (5 °C/min) to 200 °C. The inflection temperatures were determined from the scans at 20 °C. The mass losses were recorded, and a first estimation of the moisture contents was determined according to the normalized scans in which the actual mass was divided by the initial mass.

NIR Analysis. Each starch sample was placed above distilled water and then moistened with ~17% water (g/g), similar to how the NIR spectra were obtained. The spectrum of each starch sample was continuously measured through spontaneous dehydration in desiccators until each sample was dried to ~5% (g/g); the time interval between measurements was ~5 min at first and ~30 min for the final measurements.

An NIRS system (Perten DA7200, Perten Instrument AB) equipped with a ceramic reference plate was used. To minimize sampling error, all of the samples were analyzed in triplicate. Calculation of the derivative spectra and partial least-squares analysis of the spectral data were performed in Unscrambler version 9.8 (CAMO ASA, Trondheim, Norway).

Water Sorption Isotherm. Water sorption isotherms were determined gravimetrically by placing gelatinized starch samples in constant relative humidity environments, which consisted of desiccators containing saturated salt solutions: LiCl (0.113), $MgCl_2$ (0.336), CH_3COOK (0.431), NaBr (0.635), NaCl (0.757), $(NH_4)_2SO_4$ (0.824), $BaCl_2$ (0.903), and K_2SO_4 (0.98). The samples were used to produce desorption isotherms that were found to have an a_w of > 0.95. The analysis of the water sorption−desorption isotherms was performed in triplicate. Furthermore, the Guggenheim−Anderson−de Boer (GAB) equation was used to model water sorption (*27*) and to predict the monolayer water values in our studies:

$$V = \frac{W_m C k A_w}{(1 - kA_w)(1 - kA_w + CkA_w)}$$

where V is the moisture content (grams per 100 g dry sample), W_m is the monolayer moisture content (grams per 100 g dry sample), A_w is the water activity, and C and k are constants. Data were analyzed using SPSS version 16 (SPSS Inc., Chicago, IL). The GAB model was applied using nonlinear regression, and the correlation coefficient (R^2) was used to evaluate the quality of the fit.

RESULTS AND DISCUSSION

Determination of the Pasting Temperature of Corn Starch. To obtain starch samples through serial gelatinization, it is important to acquire the optimum conditions for gelatinization, which is a more complex process. The onset gelatinization temperature of starch granules in water can be measured by various indirect methods, including RVA (*28*) and DSC analysis (*24*). **Figure 1** shows the RVA pasting curves for corn starch, and the onset pasting temperature is 74 °C. A previous study proved that some leaching of amylose begins at a temperature below the gelatinization temperature because of its location in noncrystalline regions and the fact that amylose is a relatively small, linear polymer molecule that can diffuse out of granules (*29*). To obtain samples with lower degrees of gelatinization, we selected 70 °C as the heating temperature for corn starch, which was below the gelatinization temperature.

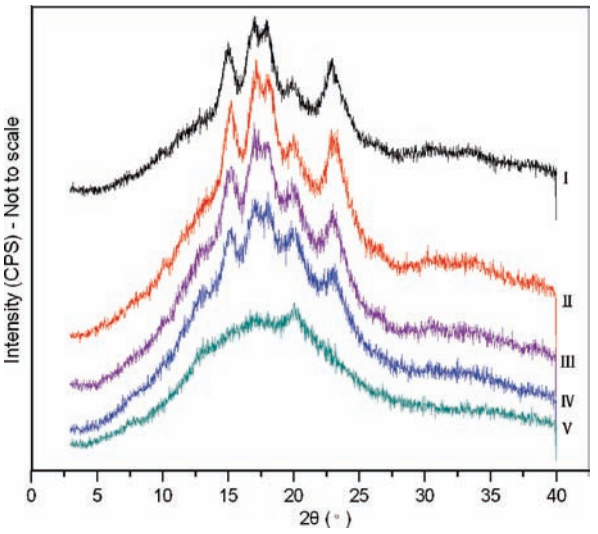

Figure 3. X-ray diffractograms of different starch samples (I−V).

Granular Changes of Heat-Treated Corn Starch. SEM pictures proved that corn starch exhibited gradual changes in granular morphology, and the outermost layers of the granules tended to maintain their integrity when the corn starch was heated for 10 min at 70 °C (**Figure 2**). As the heat treatment time increased to 15 min, dramatic changes occurred in the corn starch granules, which disintegrated as the internal structure and free movement of the starch polymers destabilized the granules' internal structure. Our observations are in agreement with those of Ratnayake and Jackson, who reported that the molecular level reorganization of the granules underwent considerable changes when corn starch was heated to temperatures below the onset gelatinization temperature (*30*). Our results also proved that the granule was completely disrupted and swollen as a plasticizer when corn starch was heated to 100 °C for 60 min.

Crystallinity Changes of Heat-Treated Corn Starch. To further explore the crystallinity changes, each gelatinized starch was analyzed by X-ray diffractometry. **Figure 3** shows the X-ray diffractograms of corn starch before and after the heating process. These results show that the crystallites were better packed and preserved when the starch was heated to 70 °C for 7 min, and the X-ray diffraction profile of gelatinized starch is distinguishable. Although the granular morphology was not affected when the heat treatment time increased to 10 min (**Figure 2C**), the melting of the starch crystallites was observed, and the degree of gelatinization increased from 33.4 to 51.3%. As the heating time increased, a more significant reduction in crystallinity was observed. Furthermore, when the corn starch was heated in water to 100 °C for 60 min, the X-ray diffraction patterns exhibited few diffraction peaks, which meant that most of the gelatinized starch sample with a degree of gelatinization of 96.8% was amorphous solid starch. These results describe the progressive morphological changes in starch crystallites when the heating temperature was below the onset gelatinization temperature. At the same time, our results also prove that gelatinization is a nonequilibrium melting process and, actually,

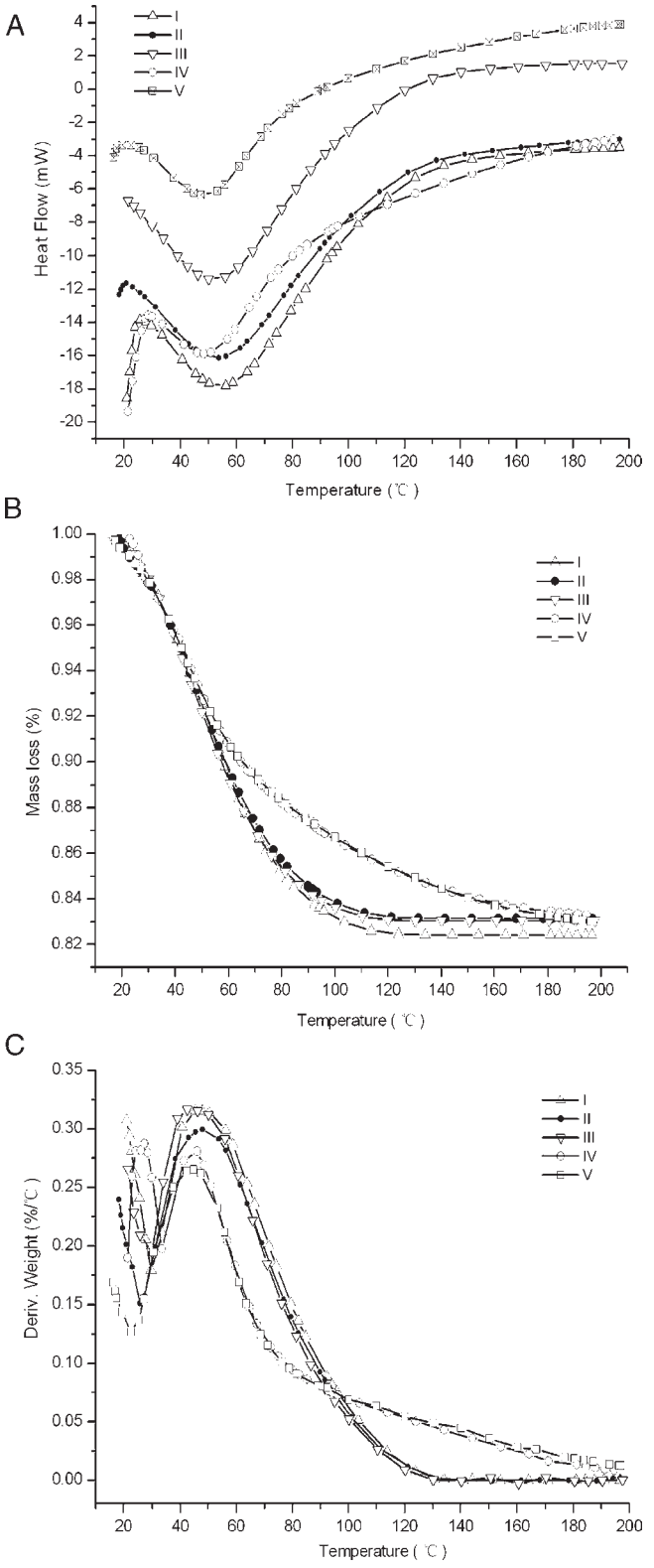

Figure 4. DSC thermograms (**A**), mass loss (**B**), and mass loss rate (**C**) measured by TG−DSC in a heating temperature range from 20 to 200 °C for different starch samples (I−V).

a continuum of relaxation processes that occur during the heating of starch in water.

Dehydration Behavior Analyzed by TG−DSC. The effect of inner structure on the dehydration behavior of gelatinized starch was studied by TG−DSC. **Figure 4A** shows DSC plots of each gelatinized starch, and the thermal studies show the same thermal stability between the native starch and each gelatinized starch, which indicates that only moisture release could contribute to weight loss in the samples. As depicted by the TG curves in **Figure 4B**, a significant loss of mass occurred before 100 °C for all kinds of corn starch samples under the same heating process. As the temperature increased above 100 °C, there was a slight decrease in mass for the native starch and gelatinized starch sample III, which ranged from 2.96 to 4.3 g/total water content (**Table 1**). However, we found that the weight losses for gelatinized starch sample IV and full gelatinized starch were 19.76 and 22.35 g/total water content, respectively.

Table 1. Distribution of Dehydration Rates Measured by TG−DSC with Heating Temperatures of 20−200 °C for Different Starch Samples (I−V)

sample	total water content (% dry base)	dehydration value I[a] (% dry base)	ratio of dehydration value I[b]	dehydration value II[c] (% dry base)	ratio of dehydration value II[d]
I	18.6	17.8 ± 0.2	95.69%	0.8 ± 0.2	4.3%
II	16.9	16.4 ± 0.2	97.04%	0.5 ± 0.2	2.96%
III	16.7	16.1 ± 0.3	96.41%	0.6 ± 0.3	3.59%
IV	16.7	13.4 ± 0.4	80.24%	3.3 ± 0.4	19.76%
V	17.0	13.2 ± 0.3	77.65%	3.8 ± 0.3	22.35%

[a] Dehydration value at heating temperatures ranging from 20 to 100 °C. The data in the column are means ± the standard deviation (SD) ($n = 3$). [b] Ratio of dehydration value I in total water content. [c] Dehydration value at heating temperatures ranging from 100 to 200 °C. The data in the column are means ± SD ($n = 3$). [d] Ratio of dehydration value II in total water content.

Figure 4C shows the dehydration rate of native starch and each gelatinized starch under the same heating process. When the heating temperature ranged from 45 to 92 °C, the dehydration rates of samples IV and V were lower than those for native starch and other partially gelatinized starches. As the temperature increased above 92 °C, the dehydration rates of samples IV and V were higher than those for other samples. In conclusion, our results show an apparent difference between the dehydration behavior of water in native starch and that in partially and fully gelatinized starch and directly prove that the inner structure of starch has a significant effect on the drying kinetics of water.

Chemometric Analysis of Gelatinized Starch. The NIR spectra of each gelatinized starch with a moisture content from 5 to 17% (g/g) after baseline corrections and normalizing pretreatments are shown in **Figure 5A**, and the first-derivative spectra are shown in **Figure 5B**. Significant differences among these spectra for each gelatinized starch are observed at ~960 and ~1491 nm, indicating that the hydrogen bond network was transformed by the modification of gelatinized starch (*31*, *32*).

The spectral vectors obtained from partial least-squares (PLS) regression analysis were directly related to the concentration of interest, and PLS was performed on each set of NIR spectra for native and gelatinized starch. The variations in the first spectral vectors of each set of starch samples extracted by PLS analysis are plotted in **Figure 5C**. The intensity of the band at 1491 nm, which was an excellent marker of the stronger hydrogen bond, decreased in gelatinized starch. It could be concluded that the stronger hydrogen band of the hydrogen bond network of water in starch decreases with the melting of crystallites. A previous study proved that water molecules are located in crystalline colloidal particles that are formed during starch synthesis (*14*). Furthermore, Imberty et al. found that half of the water molecules are tightly bound to the double helices of starch crystalline particles, and the remainder forms a complex network centered around the 6-fold screw axis of the unit cell (*33*). Thus, the disruption of both the amorphous and crystalline structures during heat treatment results in a loss of molecular order and water in crystalline starch particles, and the number of strong hydrogen bonds decreases with the melting of crystallites.

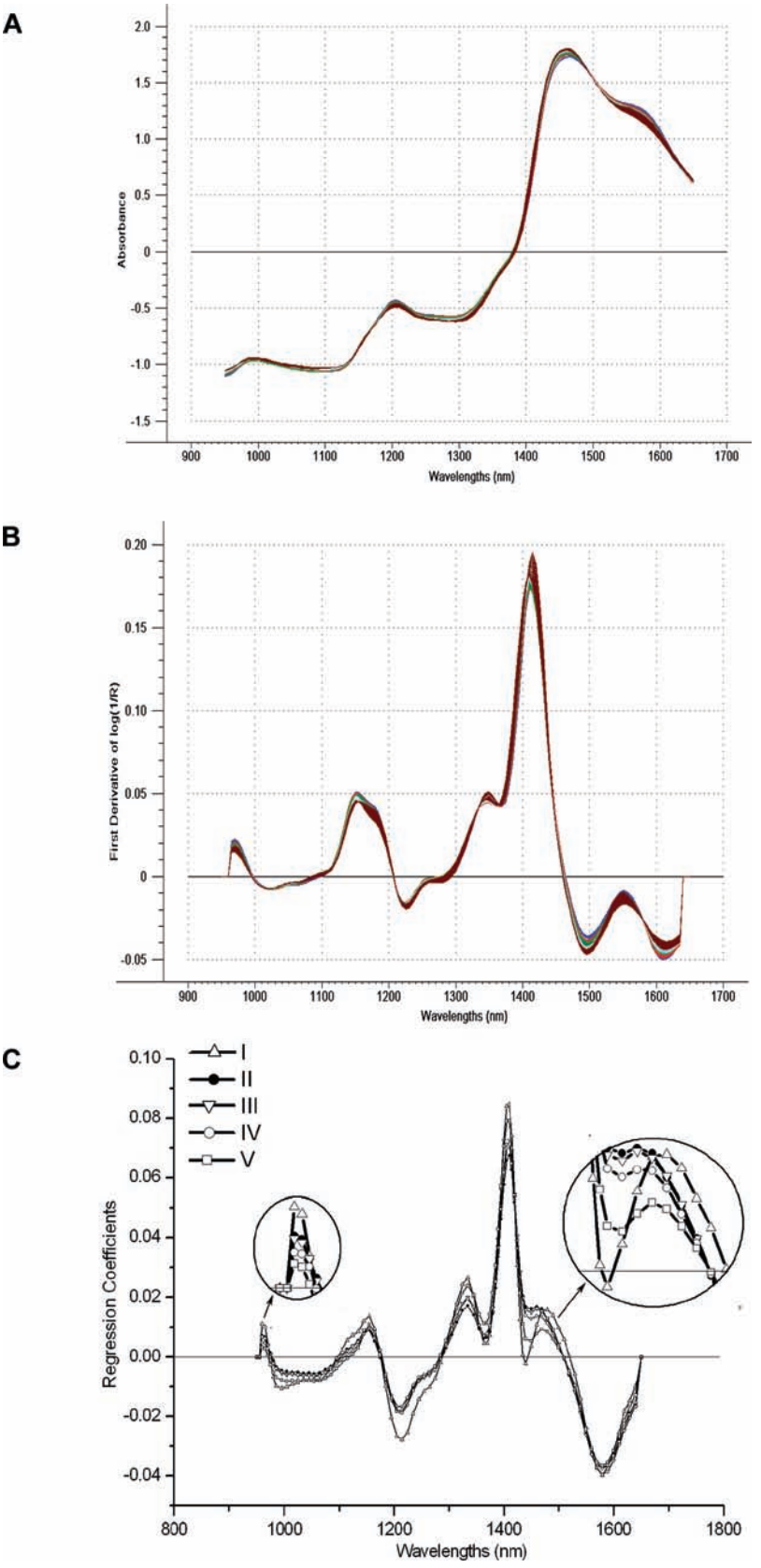

Figure 5. Set of 100 NIR spectra (**A**) and first-derivative NIR spectra (**B**) of different starch samples (I−V) containing water ranging from a level of 5 to 17% (g/g, dry base). (**C**) First PLS vector calculated from each data set of 20 NIR spectra of the different starch samples.

We also found that the intensity of the band at 960 nm decreased from native starch to sample V (**Figure 5C**). The ratio between the peak area at 1412 and 1491 nm increased. The results described above prove that the amount of free water decreases in starch, and the number of weaker hydrogen bonds in the hydrogen bond network of water increases with the melting of crystallites. In the TG−DSC analysis described above, we found that the dehydration rate decreased with an increase in the degree of gelatinization.

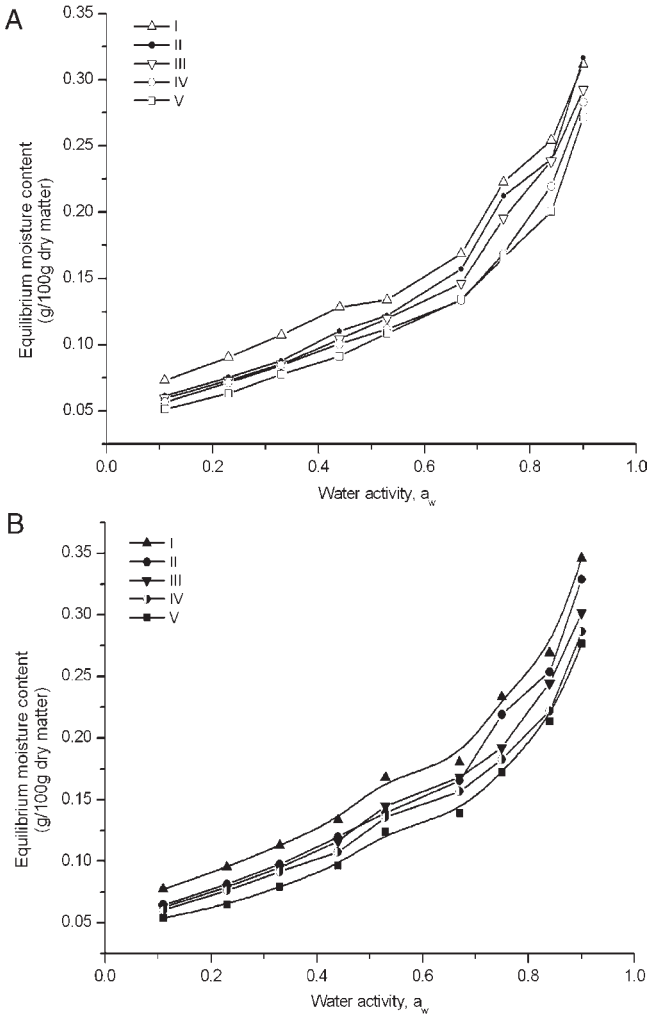

Figure 6. Isotherms of water adsorption (**A**) and isotherms of water desorption (**B**) at 25 °C for different starch samples (I−V).

The heating process likely resulted in the increase in the number of amorphous structures, which led to an increase in the number of sites and groups taking part in water binding and a decrease in condensed water capacity. In this view, more and more bound water in starches could yield a decrease in their diffusion coefficient, and the decreased diffusion velocity could impede drying because of the slower diffusion of water to the surface. Thus, the dehydration rate decreased with the increase in the degree of gelatinization.

Changes in Monolayer Water Values of Gelatinized Starch. Several mathematical models, including the GAB equation, which have been used to describe water sorption isotherms (**Figure 6**), could estimate the content of monolayer water (*34*). In our studies, the GAB equation was used to fit the experimental data of gelatinized starch, where $R^2 > 0.99$ in all cases. The parameters C, k, and W_m calculated from the GAB equation are listed in **Table 2**. The monolayer value for the native starch was higher than those of the starch samples with higher degrees of gelatinization. Our results show that the heating treatment causes a decrease in the monolayer value, which indicates the stronger affinity of monolayer water compared to multilayer and condensed water. A very similar conclusion was reached by Włodarczyk-Stasiak and Jamroz, who suggested that monolayer values decreased in starch−protein extrusions (*35*).

Furthermore, the monolayer values for starch samples with higher degrees of gelatinization of 70 and 100% were lower than

Table 2. Statistical Values of Coefficients k and C and Monolayer Water Contents of the GAB Model for Different Starch Samples

	adsorption				desorption			
sample	W_m	k	C	R^2	W_m	k	C	R^2
I	8.1	0.823	45.561	0.993	8.8	0.825	40.832	0.988
II	7.0	0.866	33.377	0.991	7.8	0.823	26.05	0.994
III	6.7	0.859	33.977	0.997	7.7	0.851	30.292	0.994
IV	5.8	0.88	115.145	0.996	7.2	0.828	32.946	0.992
V	5.7	0.875	46.692	0.994	6.9	0.837	31.048	0.994

those of native starch, which agree with the results obtained for the changes in the hydrogen bond network. To study the differences in the binding forces of water, water present in starch or food is conventionally classified into monolayer, multilayer, or condensed water. While water can be tightly bound to the double helices of crystalline starch particles, the monolayer capacities of crystalline regions could be higher than those of amorphous regions in starch. The crystallites of starch granules would be pulled apart during the heat treatment and eventually undergo hydration and melting, which are intimately related to the disruption of stronger hydrogen bonds and hydration. The gelatinization process resulted in the increase in the number of amorphous structures in the product, which led to a decrease in monolayer capacity.

In conclusion, the hydrogen bond network of water in starch, which includes strong and weak hydrogen bonds, was investigated in this work. While the magnitude of this influence on the inherent properties of starch remains debatable, it is clear that the ratio of stronger to weaker hydrogen bonds in starch is responsible for the dehydration behavior of starchy products. We also observed differences in the dehydration processes between native starch and gelatinized starch. Our data directly prove that the structure changes that occurs during heat treatment affect the availability, quality, and number of sites and groups that participate in water binding.

LITERATURE CITED

(1) Pauling, L. The adsorption of water by proteins. *J. Am. Chem. Soc.* **1945**, *67*, 555−557.
(2) Basnayake, R.; Peterson, G. R.; Casadonte, D. J., Jr.; Korzeniewski, C. Hydration and interfacial water in Nafion membrane probed by transmission infrared spectroscopy. *J. Phys. Chem. B* **2006**, *110*, 23938−23943.
(3) Elsaesser, T. Two-dimensional infrared spectroscopy of intermolecular hydrogen bonds in the condensed phase. *Acc. Chem. Res.* **2009**, *42*, 1220−1228.
(4) Wojtkow, D.; Czarnecki, M. A. Effect of temperature and concentration on the structure of tert-butyl alcohol/water mixtures: Near-infrared spectroscopic study. *J. Phys. Chem. A* **2005**, *109*, 8218−8224.
(5) Iwamoto, R.; Matsuda, T. Infrared and near-infrared spectral evidence for water clustering in highly hydrated poly(methyl methacrylate). *Anal. Chem.* **2007**, *79*, 3455−3461.
(6) Dominguez-Vidal, A.; Kaun, N.; Ayora-Canada, M. J.; Lendl, B. Probing intermolecular interactions in water/ionic liquid mixtures by far-infrared spectroscopy. *J. Phys. Chem. B* **2007**, *111*, 4446−4452.
(7) Cava, D.; Sammon, C.; Lagaron, J. M. Water diffusion and sorption-induced swelling as a function of temperature and ethylene content in ethylene-vinyl alcohol copolymers as determined by attenuated total reflection Fourier transform infrared spectroscopy. *Appl. Spectrosc.* **2006**, *60*, 1392−1398.
(8) Angell, C. A.; Rodgers, V. Near infrared spectra and the disrupted network model of normal and supercooled water. *J. Chem. Phys.* **1984**, *80*, 6245−6252.
(9) Ridi, F.; Fratini, E.; Milani, S.; Baglioni, P. Near-infrared spectroscopy investigation of the water confined in tricalcium silicate pastes. *J. Phys. Chem. B* **2006**, *110*, 16326−16331.

(10) Segtnan, V. H.; Sasic, S.; Isaksson, T.; Ozaki, Y. Studies on the structure of water using two-dimensional near-infrared correlation spectroscopy and principal component analysis. *Anal. Chem.* **2001**, *73*, 3153−3161.
(11) Stokvold, A.; Dyrstad, K.; Libnau, F. O. Sensitive NIRS measurement of increased moisture in stored hygroscopic freeze dried product. *J. Pharm. Biomed. Anal.* **2002**, *28*, 867−873.
(12) libnau, F. O.; Toft, J.; Christy, A. A.; Kvalheim, O. M. Structure of liquid water determined from infrared temperature profiling and evolutionary curve resolution. *J. Am. Chem. Soc.* **1994**, *116*, 8311−8316.
(13) BeMiller, J. N. *Carbohydrate chemistry for food scientists*; AACC International, Inc.: St. Paul, MN, 2007; pp 175−185.
(14) Walstra, P. *Physical Chemistry of Foods*; Marcel Dekker, Inc.: New York, 2003; pp 187−201.
(15) Imberty, A.; Perez, S. Conformational analysis and molecular modelling of the branching point of amylopectin. *Int. J. Biol. Macromol.* **1989**, *11*, 177−185.
(16) Imberty, A.; Chanzy, H.; Perez, S.; Buleon, A.; Tran, V. The double-helical nature of the crystalline part of A-starch. *J. Mol. Biol.* **1988**, *201*, 365−378.
(17) Corzana, F.; Motawia, M. S.; Herve du Penhoat, C.; van den Berg, F.; Blennow, A.; Perez, S.; Engelsen, S. B. Hydration of the amylopectin branch point. Evidence of restricted conformational diversity of the α-(1→6) linkage. *J. Am. Chem. Soc.* **2004**, *126*, 13144−13155.
(18) Vermeylen, R.; Derycke, V.; Delcour, J. A.; Goderis, B.; Reynaers, H.; Koch, M. H. Gelatinization of starch in excess water: Beyond the melting of lamellar crystallites. A combined wide- and small-angle X-ray scattering study. *Biomacromolecules* **2006**, *7*, 2624−2630.
(19) Calucci, L.; Galleschi, L.; Geppi, M.; Mollica, G. Structure and dynamics of flour by solid state NMR: Effects of hydration and wheat aging. *Biomacromolecules* **2004**, *5*, 1536−1544.
(20) Galamba, N.; Cabral, B. J. The changing hydrogen-bond network of water from the bulk to the surface of a cluster: A Born-Oppenheimer molecular dynamics study. *J. Am. Chem. Soc.* **2008**, *130*, 17955−17960.
(21) Hansen, P. I.; Larsen, F. H.; Motawia, S. M.; Blennow, A.; Spraul, M.; Dvortsak, P.; Engelsen, S. B. Structure and hydration of the amylopectin trisaccharide building blocks: Synthesis, NMR, and molecular dynamics. *Biopolymers* **2008**, *89*, 1179−1193.
(22) Fayer, M. D.; Levinger, N. E. Analysis of water in confined geometries and at interfaces. *Annu. Rev. Anal. Chem.* **2010**, *3*, 89−107.
(23) Levy, Y.; Onuchic, J. N. Water mediation in protein folding and molecular recognition. *Annu. Rev. Biophys. Biomol. Struct.* **2006**, *35*, 389−415.
(24) Zaidul, I. S. M.; Nik Norulaini, N. A.; Mohd. Omar, A. K.; Yamauchi, H.; Noda, T. RVA analysis of mixtures of wheat flour and potato, sweet potato, yam, and cassava starches. *Carbohydr. Polym.* **2007**, *69*, 784−791.
(25) Xiong, Y.; Bartle, S. J.; Preston, R. L. Improved enzymatic method to measure processing effects and starch availability in sorghum grain. *J. Anim. Sci.* **1990**, *68*, 3861−3870.
(26) ISO, Method 1666. Starches: Determination of moisture content—oven-drying method. **1996**.
(27) Van den Berg, C. Description of water activity of foods for engineering purposes by means of the G.A.B. model of sorption. In *Engineering Science in the Food Industry*; McKenna, B. M., Ed.; Elsevier Applied Science: London, 1984; pp 311−321.
(28) Shi, Y. C. Two- and multi-step annealing of cereal starches in relation to gelatinization. *J. Agric. Food Chem.* **2008**, *56*, 1097−1104.
(29) Airaksinen, S.; Karjalainen, M.; Shevchenko, A.; Westermarck, S.; Leppanen, E.; Rantanen, J.; Yliruusi, J. Role of water in the physical stability of solid dosage formulations. *J. Pharm. Sci.* **2005**, *94*, 2147−2165.
(30) Ratnayakea, W. S.; Jackson, D. S. A new insight into the gelatinization process of native starches. *Carbohydr. Polym.* **2007**, *67*, 511−529.
(31) Collman, J. P.; Decreau, R. A.; Dey, A.; Yang, Y. Water may inhibit oxygen binding in hemoprotein models. *Proc. Natl. Acad. Sci. U.S.A.* **2009**, *106*, 4101−4105.
(32) Headrick, J. M.; Diken, E. G.; Walters, R. S.; Hammer, N. I.; Christie, R. A.; Cui, J.; Myshakin, E. M.; Duncan, M. A.; Johnson, M. A.; Jordan, K. D. Spectral signatures of hydrated proton vibrations in water clusters. *Science* **2005**, *308*, 1765−1769.
(33) Imberty, A.; Perez, S. A revisit to the three-dimensional structure of B-type starch. *Biopolymers* **1988**, *27*, 1205−1221.
(34) Sato, Y.; Wada, Y.; Higo, A. Relationship between monolayer and multilayer water contents, and involvement in gelatinization of baked starch products. *J. Food Eng.* **2010**, *96*, 172−178.
(35) Włodarczyk-Stasiak, M.; Jamroz, J. Analysis of sorptin properties of starch-protein extrudates with the use of water vapour. *J. Food Eng.* **2008**, *85*, 580−589.

Received for review September 14, 2010. Revised manuscript received November 16, 2010. Accepted November 16, 2010.